journal

J. Am. Ceram. Soc., 78 [1] 121-28 (1995)

Low-Temperature Sinter Forging of Nanostructured Y-TZP and YCe-TZP

Michel M. R. Boutz, Louis Winnubst,*,† and Antonie J. Burggraaf

Laboratory for Inorganic Chemistry, Materials Science and Catalysis, Faculty of Chemical Technology, University of Twente, 7500 Enschede, The Netherlands

Marco Nauer‡ and Claude Carry*,§

Laboratoire de Céramique, Ecole Polytechnique Fédérale de Lausanne, CH-1015 Lausanne, Switzerland

Compacts of ultrafine Y-TZP and YCe-TZP powders have been sinter forged under constant load at low temperatures (1100°–1200°C). The application of a uniaxial load leads to a strong reduction in sintering time, which in combination with the virtual absence of dynamic grain growth makes it possible to effectively limit grain growth. Nanostructured (grain size 100 nm) TZP with high relative densities (90%–93%) could thus be produced by sinter forging under 84 MPa at 1100°C. The contributions of both creep and densification to the dimensional changes of the sinter-forging samples have been analyzed. A strong reduction of the flaw concentration was observed in sinter-forged materials as compared to freely sintered ones.

I. Introduction

The intrinsic driving force for densification is often represented by the so-called sintering pressure. This sintering pressure is inversely proportional to both particle size and pore radius.[1] To obtain a high intrinsic driving force therefore requires compacts of ultrafine powders with small average pore radii. The application of an external pressure acts as an additional driving force for densification,[2] which can be used to further reduce sintering time and temperature.

If agglomerates, which are present in the starting powders, cannot be broken during the formation of the green body, they will cause the existence of regions sintering at a different rate than the surrounding matrix during high-temperature consolidation. This so-called differential sintering leads to incompatibility stresses that can ultimately lead to the opening of microcracks around these regions. These incompatibility stresses can be relieved only by plastic deformation of the matrix material.[3] Flaws, introduced during the formation of the green body due to, for example, binder burnout or inhomogeneous compaction, can likewise be eliminated by deforming the material during densification. This leads to a considerable improvement of the final mechanical properties if the plastic strain surpasses a certain limit as shown by Venkatachari and Raj[4] in the case of alumina.

There are three main techniques of pressure-assisted sintering.

(a) Hot isostatic pressing (HIPing). A hydrostatic gas pressure is applied to the specimen and the shrinkage is isotropic; i.e., no permanent shape change occurs.

(b) Hot pressing. A uniaxial pressure is applied to a powder, which is constrained in the lateral direction by the die wall. The radial strain thus equals zero and the unknown parameter is the stress, exerted by the die walls on the specimen, trying to expand.

(c) Sinter forging. A uniaxial pressure is applied again, but the sample is free to move in the lateral direction. The radial strain can be negative or positive, depending on the relative magnitude of sintering and creep.

During free sintering and HIPing, the macroscopic plastic strain is zero. However, at the microscopic level, shear stresses and strains do exist.[5] The plastic strain is directly related to the volumetric strain during hot pressing. Only in the case of sinter forging is the processing path (volumetric strain versus plastic strain) not fixed, and the amount of plastic strain suffered by the specimens upon reaching their final density can be varied by changing the magnitude of the applied stress (see Fig. 3 in Ref. 4 for a graphical illustration of different processing paths). This offers the opportunity to impose large plastic strains on the material during densification and effectively eliminate residual flaws.

During sinter forging of fine-grained ceramics, creep often occurs via grain boundary sliding. It has been shown that for real microstructures substantial shear deformation occurs locally.[6] This shear deformation can lead to pore flattening and finally pore closure. Furthermore, the shear deformation occurring at the grain boundaries during sinter forging can result in removal of a glassy phase and elimination of defects. The macroscopic mechanical properties of the material are improved by the reinforcement of the grain boundaries.[7]

In this paper, the sinter-forging characteristics at low temperatures (1100°–1200°C) of compacts of ultrafine Y-TZP and YCe-TZP (tetragonal zirconia polycrystals) powders will be described. It will be investigated whether sintering time and temperature can be reduced to such an extent that the grain size remains in the nanometer regime (≤100 nm), when the materials reach high densities. Both decreasing the grain size and codoping with ceria increase the aging resistance of Y-TZP.[8] The dependence of both creep and densification rates on the applied stress has been analyzed, using the approach proposed by Raj.[9] For this purpose, the density and radial strain have been monitored by means of interrupted tests. The flaw populations of sinter-forged and free-sintered bodies will be compared, and the importance of creep strain for flaw elimination will be examined.

II. Experimental Procedure

Ultrafine tetragonal zirconia powders with different amounts of yttrium and cerium have been synthesized by a gel precipitation technique using metal chlorides as precursor chemicals. Details of this so-called chloride method can be found elsewhere.[10] The nominal chemical composition of the synthesized

I-W. Chen—contributing editor

Manuscript No. 193752. Received March 14, 1994; approved July 5, 1994.
Supported by Akzo Chemicals B.V., Amsterdam, The Netherlands.
*Member, American Ceramic Society.
†Author to whom correspondence is to be addressed.
‡Present address: Moldinject, Fabrikstrasse 23, CH 3250 Lyss, Switzerland.
§Present address: Institut de Sciences des Materiaux (I.A.M.A.), Université de Paris-Sud Centre d'Orsay, F 91405 Orsay Cedex, France.

powders can be found in Table I. All powders have an initial crystallite size of 8–9 nm (surface areas of 105–120 m^2/g).

Two specimen geometries have been used for sinter-forging tests: cylindrical and rectangular. Cylindrical specimens were made by cold isostatic compaction in two steps (100 MPa, followed by 400 MPa). Rectangular specimens were made by cold uniaxial compaction at 50 MPa in a steel die (40 mm × 8 mm), followed by isostatic compaction at 400 MPa.

Cylindrical specimens with height/diameter ratios 2.2–2.5 were used to analyze the sinter-forging kinetics at 1100°C by means of interrupted tests. Rectangular specimens were sinter forged at higher temperatures (1150°–1200°C) into a platelike shape with near-theoretical densities.

Before sinter forging, all specimens were presintered by heating at 120°C/h to 950°C, immediately followed by cooling at 60°–120°C/h. This resulted in a slight increase in density from 45% to 48.0%–48.5%, but more importantly the accessible surface area decreased dramatically from >100 m^2/g to 20 m^2/g. Since the porosity is open at such low densities, the decrease in surface area is caused by a strong increase of the fractional neck area, thereby improving the strength and thermoshock resistance of the specimens.

After this presintering step, the specimens were machined to their appropriate dimensions. Cylindrical specimens had the following dimensions (height × diameter): 15.7 mm × 7.3 mm (ZY5) or 17.3 mm × 7.0 mm (ZY4Ce4). Rectangular specimens had the dimensions ($l_x \times l_y \times l_z$) 15 mm × 6 mm × 8 mm (ZY5) or 15 mm × 6 mm × 6 mm (ZY4Ce2).

Sinter-forging tests were performed in air at 1100°–1200°C under constant load, using either a screw-driven testing machine (model 1361, Instron, Great Britain) or an hydraulic compression machine (Elatec, Finland). Both machines are equipped with SiC rods. Axial displacements are measured *in situ* during all tests, and specimen temperatures were monitored by a thermocouple located in the immediate vicinity of the forging specimens. The hydraulic machine is connected to a controller (model FICS-11, Eurotherm, The Netherlands) and a computer equipped with a supervisory software package (ESP, version 3.22, Eurotherm, The Netherlands) in a master–slave configuration. A cascade control system (master: load, slave: hydraulic pressure) enables the performance of constant-load experiments.

During the tests performed at 1100°C on cylindrical specimens, polished sapphire disks were used to reduce friction and to avoid direct contact between specimen and SiC rods. Polished SiC loading pads were used during tests performed at 1150° and 1200°C on rectangular samples. Sinter-forging tests of ZY5 at 1100°C have been performed with the screw-driven machine, while all other tests were done with the hydraulic machine. Both machines gave comparable results during creep tests of ZY5, indicating that identical testing conditions could be used on both machines.

The same heating schedule has been used during all sinter-forging tests: heating to 950°C at 600°C/h, followed by heating to the end temperature (1100°, 1150°, or 1200°C) at 300°C/h. During the last heating segment, the presintered specimens start to densify again. Shrinkage occurs both in axial and radial directions. Because strains are defined with respect to the dimensions before testing (see below), the radial shrinkage during heating can lead to a negative value of the radial strain at the moment densification starts.

Table I. Composition of Investigated Powders

Code	Composition (mol%)		
	ZrO_2	$YO_{1.5}$	CeO_2
ZY5	95	5	
ZY4Ce2	94	4	2
ZY4Ce4	92	4	4

During sinter forging at 1100°C of ZY5 and ZY4Ce4, three different loads, 1000–2000–3000 N, have been used to compress the cylindrical samples. The applied loads resulted in initial stresses (calculated using the diameters observed at the moment the load has just reached its final value) of 28–58–84 MPa and 29–57–84 MPa in the case of YZ5 and ZY4Ce4, respectively. Once the end temperature (1100°C) was reached during these tests, the load was increased to its final value within 200 s and then kept constant. The maximum compression duration at this temperature was 185 min.

During sinter forging at 1150° and 1200°C, rectangular specimens were compressed under a constant load, corresponding to an initial stress (σ_i) of 80 MPa (calculated using the dimensions before testing). The load was imposed on the 15 mm × 6 mm side of the specimens. In most of these tests, the load was raised in a linear way to its final value during heating from 950°C to the end temperature (1150°/1200°C). Upon reaching the end temperature, the load was kept constant for 25 min.

The axial displacements Δh were taken from the internal LVDT (linear voltage displacement transducer), while the radial displacements of cylindrical samples were calculated from the mass, height, and final density of the specimens after interrupted tests.

The procedure outlined by Raj[9] has been used to separate creep and densification, which occur simultaneously during sinter forging. The uniaxial plastic strain in the z (compression) direction ε_c, hereafter referred to as creep strain, is defined herein for a cylindrical specimen geometry as

$$\varepsilon_c = 2/3 \mid \varepsilon_z - \varepsilon_r \mid = \mid \varepsilon_z - (\varepsilon_v/3) \mid \quad (1)$$

where ε_z, ε_r, and ε_v are the axial, radial, and volumetric strain. All strains have been calculated with the starting dimensions (before testing) as reference values.

Friction at the loaded ends of the specimens may influence the stress distribution and resulting deformation.[11] This friction can lead to barreling of cylindrical specimens. The amount of barreling has been found to be insignificant under the investigated experimental conditions. The difference between the diameter at the end of the specimen and the average diameter (as calculated from the mass, height, and density of the specimens) was generally less than 2%. The use of sapphire disks during sinter forging of cylindrical samples thus leads to a satisfactory reduction of friction at the loaded ends.

SiC loading pads were used for sinter forging of rectangular samples ($l_x \times l_y$ = 15 mm × 6 mm, l_z = 6 or 8 mm). There was considerable friction between the specimen and loading pads, as will be further discussed in Section III(2). A large difference in relative expansion of the sinter-forged specimens along the x (length) and y (width) axis has been observed. The ratio in the true strains in the x- and y-direction varied between 1.3 and 3.5. This multiaxial strain state has been converted into an equivalent uniaxial strain ε_e using

$$\varepsilon_e = \frac{2}{3}\sqrt{\frac{1}{2}[(\varepsilon_x - \varepsilon_y)^2 + (\varepsilon_y - \varepsilon_z)^2 + (\varepsilon_z - \varepsilon_x)^2]} \quad (2)$$

where ε_x, ε_y, and ε_z are the true strains in x, y, and z direction.

Densities were measured by the Archimedes technique (in Hg). Nitrogen adsorption/desorption isotherms were obtained at 77 K (model ASAP 2400, Micromeritics, Norcross, GA). Specific surface areas were determined by the BET method (no corrections for microporosity were necessary).

The free sintering behavior of the investigated TZPs has been analyzed by means of dilatometry (model 402E, Netzsch, Germany). Density was calculated from the initial value and the observed axial shrinkage. Corrections for weight loss (due to evaporation of adsorbed water) and thermal expansion of the samples were applied. Grain sizes D were determined by the lineal intercept technique from SEM (Hitachi S800) micrographs of polished, thermally etched cuts using $D = 1.56\ L$, where L is the average lineal intercept, corrected for the presence of residual porosity using the method described by Wurst and Nelson.[12]

III. Results

(1) Sinter Forging Kinetics at 1100°C

The increase in relative density with time during sinter forging and free sintering at 1100°C is shown in Figs. 1(a) and (b) for ZY5 and YZ4Ce4, respectively. Clearly, the application of a uniaxial stress has a strong beneficial effect on the densification kinetics of both zirconia materials. It can also be seen that ZY5 densifies slower than ZY4Ce4 during free sintering, while the reverse is true during sinter forging.

Final densities equal 93%–94% for the sinter-forged ZY5 samples, while the free-sintered sample reaches only 84% after 10 h. During sinter forging under 84 MPa initial stress, only 22 min is needed to reach 93%. Prolonged sinter forging (160–185 min) under initial stresses of 58 and 84 MPa did not increase the density any further, indicating that at 94% relative density creep proceeds at constant porosity. Some results of ZY4Ce4 and ZY4Ce2 are the same. The material then has the code YCe-TZP. During free sintering of YCe-TZP, more than 10 h is required to reach 90% relative density, while during sinter forging only 100, 50, or 30 min is needed under 29, 57, and 84 MPa, respectively. Unlike ZY5, where final densities obtained through sinter forging remained below 95%, a relative density of 97% could be reached during sinter forging of ZY4Ce4 under 84 MPa for 2 h. By raising the temperature for sinter forging to 1150°C, densities of 96%–99% are obtained in 25 min under 80 MPa for both zirconia materials (Section III(2)).

The observed time dependence of the resulting stress during the constant-load experiments was as follows for both investigated materials: under the 2000- and 3000-N loads, the stress decreases continuously, due to radial expansion of the specimens, while under 1000-N load the stress remains essentially constant at its initial value (28, 29 MPa). The observed variation in diameter is very small under the 1000-N load. Contraction, due to sintering, is balancing here with expansion, due to creep.

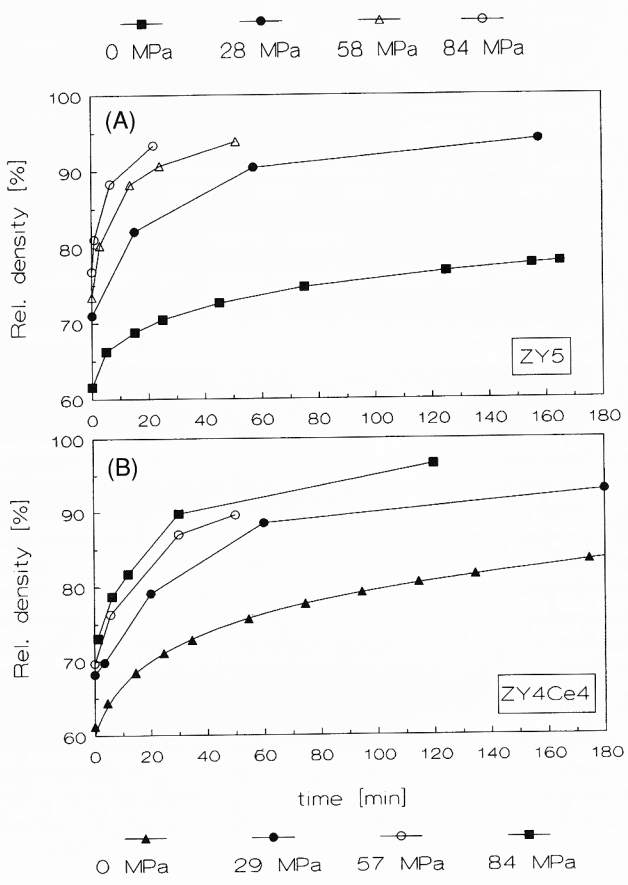

Fig. 1. Increase of relative density with time at 1100°C during free sintering (0 MPa) and sinter forging of (A) ZY5 and (B) ZY4Ce4. Initial stresses used for sinter forging are indicated in the legends.

Grain sizes, together with other relevant data of the specimens sinter forged at 1100°C, are shown in Table II. An average grain size of 0.10 μm is observed in the 93% dense ZY5 and the 90% dense YCe-TZP specimen sinter forged under 84 MPa. During sinter forging of ZY5 with constant displacement rate at 1100°C, a density of 93% with a grain size of 0.13 μm was obtained after 23 min by an initial strain rate of $3 \times 10^{-4}\ s^{-1}$ (piston displacement rate of 0.2 mm/min). The final stress is approximately 200 MPa at the end of this test.

Furthermore, it is evident from the data presented in Table II for the 84 MPa experiments, that grain growth during sinter forging is very sluggish at 1100°C. No difference in grain size had been observed between specimens sinter forged or free sintered for equal times at 1100°C, indicating the virtual absence of dynamic grain growth under the investigated experimental conditions.

In Figs. 2(a) and (b) the creep strain is given as a function of time for both sets of experiments. The creep rate of ZY5 is significantly higher than that of ZY4Ce4. In Figs. 3(a) and (b) the processing paths ε_v versus ε_c are shown for both materials. It can be seen that the amount of creep strain suffered by the materials upon reaching a particular density (and hence a particular volumetric strain) depends on the magnitude of the applied stress. For instance, in the case of ZY5 upon reaching the end density (94%) the specimen has undergone a creep strain of 0.26 under 28 MPa, while the creep strain increases to 0.42 by increasing the applied stress to 84 MPa. As mentioned before, a transition to pure creep occurs for ZY5 after reaching 94% relative density. Comparing the processing paths of both TZPs, it can be seen that at a given creep strain ZY5 has attained a higher volumetric strain and hence a higher density than ZY4Ce4, independent of the applied stress.

The stress dependence of the creep rate during sinter forging has been analyzed assuming the relation $\dot{\varepsilon}_c \sim \sigma_e^n$ holds, where n is the creep stress exponent. The internal load-bearing area changes continuously during sinter forging and with it the stress intensification factor ϕ, defined as the ratio of the external cross-sectional area of the specimen and its effective internal load-bearing area. Various expressions have been proposed for ϕ (reviews can be found in Refs. 2 and 13), depending on the assumed pore and grain geometry. However, all these expressions contain only the porosity P as an independent variable. For instance, Coble[2] suggested that $\phi = 1/(1 - P)$ is the correct expression for diffusion models of hot pressing. Therefore, taking the strain rates at constant density for the sinter-forging specimens ensures that the stress intensification factor is constant. In Fig. 4, the stress dependence of the creep rate is shown in a double-logarithmic plot. The creep rate has been calculated at 85% and 90% relative density for ZY5 and at 80% and 85% relative density for ZY4Ce4. In the case of ZY5, the stress exponent n, as calculated from the slope of the curves, equals 2.5 at both density values. In the case of ZY4Ce4, the stress exponent is significantly lower; it is equal to 1.6 and 1.5 at 80% and 85% relative density, respectively. The observed creep rates are highest for ZY5 and are of the order of 10^{-5}–$10^{-4}\ s^{-1}$. Such strain rates are typical for superplastic forming of ceramics, but are normally obtained only at temperatures well above 1100°C.

(2) Sinter Forging at 1150°–1200°C

Rectangular specimens of ZY5 and ZY4Ce2 have been sinter forged at 1150° and 1200°C for 25 min under a constant load corresponding to an initial stress of 80 MPa into a platelike shape. As mentioned in Section II, the relative expansions of these sinter-forged specimens in the x (length) and y (width) direction were quite different ($\varepsilon_x << \varepsilon_y$). Since these rectangular specimens shrank isotropically during free sintering, the observed anisotropic deformation must be due to strong friction

Table II. Relevant Data (Sinter Forging Conditions, Final Densities, Creep Strains, and Grain Sizes) of TZP Sinter Forged at 1100°C

Composition	σ_0 (MPa)	Duration (min)	ρ_{rel} (%)	ε_c	D (μm)
ZY5	28	158	94	0.26	0.14
ZY5	84	22	93	0.42	0.10
ZY5	84	185	94	0.97	0.15
ZY4Ce4	29	180	93	0.29	0.14
ZY4Ce4	57	50	90	0.36	0.12
ZY4Ce4	84	1	73	0.20	0.06
ZY4Ce4	84	30	90	0.42	0.10
ZY4Ce4	84	120	97	0.57	0.14

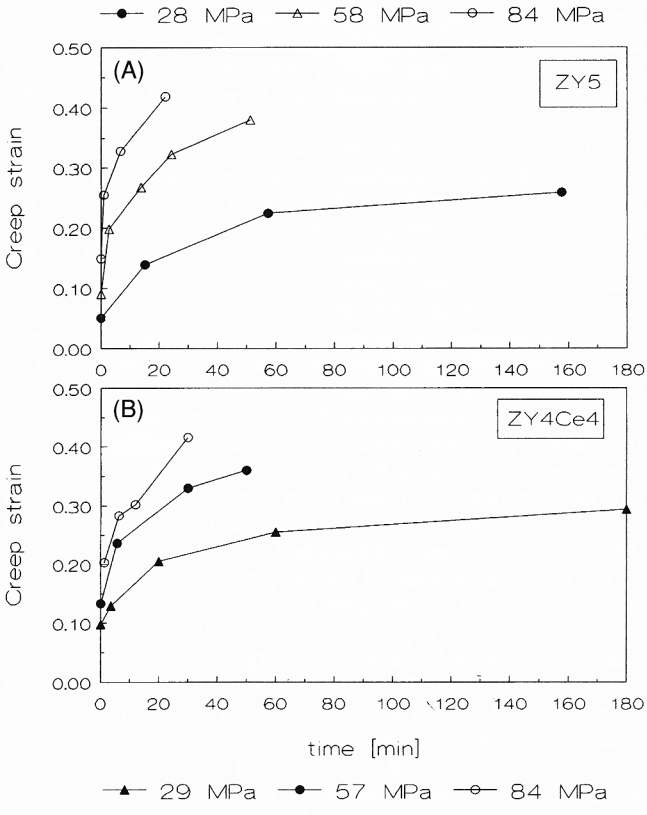

Fig. 2. Increase of creep strain with time during sinter forging at 1100°C of (A) ZY5 and (B) ZY4Ce4.

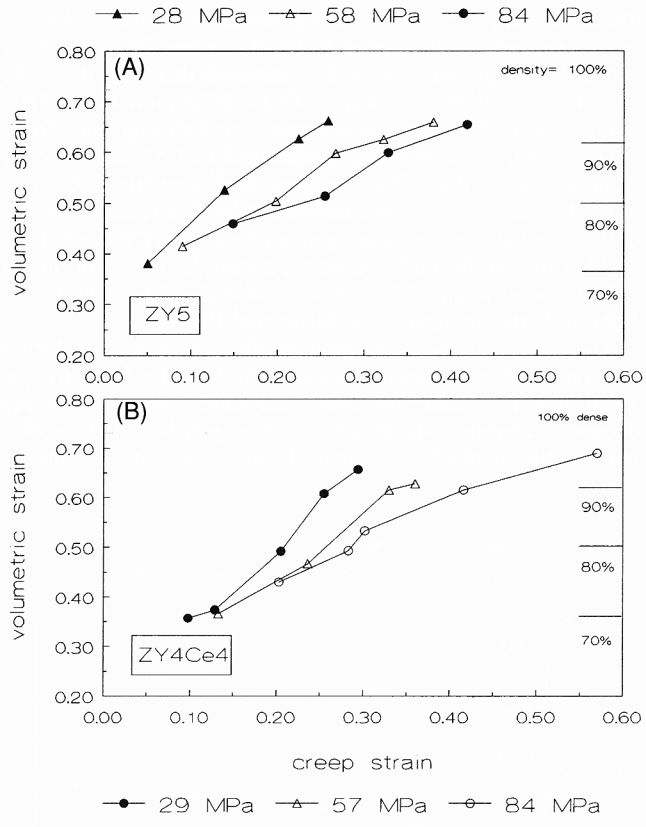

Fig. 3. The processing path ε_v versus ε_c of the sinter-forging experiments conducted at 1100°C on (A) ZY5 and (B) ZY4Ce4.

between the loaded ends of the specimens and the loading pads. He *et al.*[14] observed a 40-μm-thick porous layer at the loaded ends of ZTA (zirconia toughened alumina) plates sinter forged with the same equipment and loading configuration as in the present paper; this clearly indicates strong friction conditions at the specimens' ends during these "plate-forging" tests. The multiaxial strain state of the sinter-forged plates has been converted into an equivalent uniaxial strain ε_e (Eq. (2), Section II), hereafter referred to as effective strain.

The relevant data (grain size, strains, densities) of these tests are summarized in Table III. Densities of 96%–99% of the theoretical one have been obtained. These specimens have undergone extensive deformation, since effective strains equal 0.5–0.7 at 1150°C and 0.8 at 1200°C (at 1100°C ε_c equals 0.4 after a similar stress/time profile).

Grain sizes and densities of the ZY4Ce2 material pressureless sintered at 1200°C (heating rate 120°C/h) during 0, 5, and 10 h are also given in Table III. From this table, it can be seen that some dynamic grain growth is possibly taking place during sinter forging of YCe-TZP at 1200°C, since in the sinter-forged material the grain size equals 0.25 μm after 25 min, while during free sintering the grain size is still only 0.23 μm after 600 min. A more extensive analysis of grain growth during compressive deformation of YCe-TZP is needed, however, to establish this more firmly.

While densities of 96%–99% are obtained after sinter forging at 1150° and 1200°C, free sintering usually leads to somewhat lower densities (95%–97%) at these temperatures. This 3%–5% residual porosity in free-sintered materials consists mainly of very large pores with dimensions up to 200–250 μm, which are virtually eliminated in the sinter-forged materials (see Section III(3)).

(3) Flaw Populations

The microstructures of the investigated TZPs sinter forged or free sintered to densities above 90%, where the porosity is closed, have been examined by SEM. Venkatachari and Raj[4] observed, using SEM in the case of alumina, that, in the final stage of densification, pores with sizes exceeding the mean grain size ("flaws") are fragmented into smaller ones and gradually disappear with increasing strain during sinter and hot forging. No attempt has been made in this investigation to perform a statistically sound analysis of the effect of the applied strain on

Table III. Relevant Data (Sintering and Sinter Forging Conditions, Final Densities, Axial and Effective Strains, Grain Sizes) of Sinter-Forged and Free-Sintered TZPs

Composition	Sample no.	PS/SF†	T (°C)	Time (min)	ρ_{rel} (%)	$-\varepsilon_z$	ε_e	D (μm)
ZY5	1	SF	1150	25	97	0.94	0.71	0.18
ZY5	2	SF*	1150	25	99	0.84	0.60	0.16
ZY4Ce2	3	SF*	1150	25	96	0.71	0.49	nd‡
ZY4Ce2	4	SF	1150	25	97	0.84	0.62	nd
ZY4Ce2	5	SF	1200	25	98	1.05	0.84	nd
ZY4Ce2	6	SF	1200	25	99	1.05	0.83	0.25
ZY4Ce2	7	PS	1200	0	95			0.19
ZY4Ce2	8	PS	1200	300	96			0.20
ZY4Ce2	9	PS	1200	600	96			0.23

†SF: sinter forged for 25 min under a constant load corresponding with an initial stress of 80 MPa, the load being slowly raised to its final value during heating from 950°C to the end temperature. SF*: as SF, but the load was increased in 5 min to its final value after having reached the end temperature. PS: pressureless sintered, heating rate 120°C/hr. ‡nd: not determined; these specimens were annealed at 1400°C after sinter forging in order to increase their toughness.

the flaw populations in the sinter-forged TZPs. However, several qualitative conclusions can still be drawn from SEM inspection of polished cuts of the sinter-forged and free-sintered TZPs.

The SEM analysis showed, in the ZY5 materials sinter forged to 93%–94% relative density at 1100°C (Section III(1)), that (a) the size and number of flaws decrease with increasing load (which is accompanied by an increase in creep strain), (b) the majority of the residual pores are smaller than the mean grain size and their average size is observed to decrease with increasing load, (c) densification takes place homogeneously throughout the sample during sinter forging under 58 and 84 MPa, while regions with higher density than the surrounding matrix are observed in the material sinter forged under 28 MPa. It has furthermore been found that residual flaws are still not completely eliminated even at creep strains of 0.6 in Y-TZP and YCe-TZP sinter forged at 1100°C. This is in contradiction with the prediction of Budiansky *et al.*, who stated that flaws will be eliminated at strains of 0.6. By raising the temperature for sinter forging to 1150°C, a virtually complete elimination of flaws has been accomplished for both TZPs (see below).

During sinter forging at 1100°C, creep rates of 1×10^{-5}–4×10^{-4} s^{-1} have been observed in this investigation (Fig. 4). Cavitation could possibly occur under such conditions of high strain rate at low temperature in TZP ceramics. To evaluate whether this process is really taking place, ZY5 samples sintered to 95.0% ± 0.4% relative density at 1150°C (grain size 0.2 μm) were compressed under constant load to various strains at 1100°C. Primarily because of its larger grain size and to a lesser extent because of its higher density, an initial flow stress of 355 MPa was required to obtain a strain rate of 6×10^{-5} s^{-1}, compared to approximately 50 MPa for the 90% dense sinter-forging material with a grain size of 0.1 μm. To correct for the variation in initial density (ρ_0) of the specimens before compression, the change in density after compressive deformation ($\Delta\rho$) has been normalized with respect to the initial density. The normalized change in density $\Delta\rho/\rho_0$ as well as the observed strain rates is shown in Fig. 5 as a function of the axial strain. It can be seen that the density after deformation is always higher than the initial one, but a maximum is observed in the $\Delta\rho/\rho_0$ versus ε_z curve at strains ≥0.3. This seems to indicate that partial healing of residual pores due to the imposed strain is still taking place, but simultaneously new "cavities" are nucleating, leading to a competition with regard to densification. Clearly, more work is needed to understand cavitation during compressive deformation at the studied temperatures.

At 1150°C, densities ≥95% can be obtained by free sintering for several hours with all investigated TZPs.[15] As mentioned in Section III(2), 96%–99% dense specimens can be produced by sinter forging for 25 min under an initial stress of 80 MPa at this temperature. The flaw populations of ZY5 after free sintering and sinter forging at 1150°C have been examined by SEM. In Fig. 6, representative micrographs of these materials are shown. It can be seen in Figs. 6(a) and (b) that very large flaws with dimensions up to 200–250 μm are present in the free-sintered material, while Fig. 6(c) shows that such large flaws are absent in the sinter-forged one. Only pores with dimensions smaller than the average grain size can be found in the latter material (Fig. 6(d)).

Elimination of residual porosity due to the strains imposed on Y-TZP samples during superplastic compressive deformation has also been noticed as described elsewhere.[16] Y-TZP materials sintered at 1150°C to 97% relative density showed an increase in density to 98%–99.5% after compressive deformation to 0.5 true strain at 1200°–1300°C. Specimens that received an identical heat treatment without any applied stress showed no or very little change in density.

IV. Discussion

Comparing the density evolution during free sintering and sinter forging of, for example, ZY5 at 1100°C (Fig. 1) shows that the time needed to reach a certain density value is reduced by a factor 20–600 by applying an initial stress equal to 28–84 MPa. This drastic reduction in processing time, together with the virtual absence of dynamic grain growth at this temperature (see Section III(1)), makes it possible to limit grain growth effectively. In this way the grain size of both Y-TZP (ZY5) and YCe-TZP could be kept within the nanometer regime ($D \leq 100$ nm), while simultaneously attaining high density (90%–93%) during sinter forging under the initial stress of 84 MPa.

Recently, Y-TZP powders have been synthesized by us via a hydrothermal route.[17] The sinterability of this hydrothermally prepared material is markedly better than the Y-TZP material investigated in this paper. This allowed the production of dense (95% or more) bodies with grain sizes of 80–100 nm by sinter forging at 1050°C under moderate stresses (74–84 MPa). This result, together with those presented in this paper, illustrated that sinter forging is an attractive method to produce defect-poor nanostructured materials.

It has been observed in this investigation that the creep strains imposed on TZP ceramics during sinter (or hot) forging are effective in eliminating residual flaws. The size and number of flaws were observed to decrease with increasing creep strain. Kellett and Lange[18] also observed a progressive closure of large pores with increasing creep strain during hot forging of ZTA. Near-theoretical densities could be obtained by sinter forging both investigated TZPs at 1150°–1200°C, while maintaining a very fine grain size (0.16–0.25 μm). The elimination of flaws leads to a significant improvement of mechanical properties compared to free-sintered materials, as reported by Winnubst *et al.* in the case of sinter-forged ZTA ceramics[7] and by Venkatachari and Raj in the case of alumina.[4]

Y-TZP is an oxygen-ion conductor and can be used as a solid electrolyte in solid oxide fuel cells operating at temperatures of 1000°C. The resistance of the solid electrolyte layer should be as low as possible to minimize ohmic losses in these devices. A large contribution to the total electrical resistance of fine-grained Y-TZP comes from the grain boundaries. Sinter forging

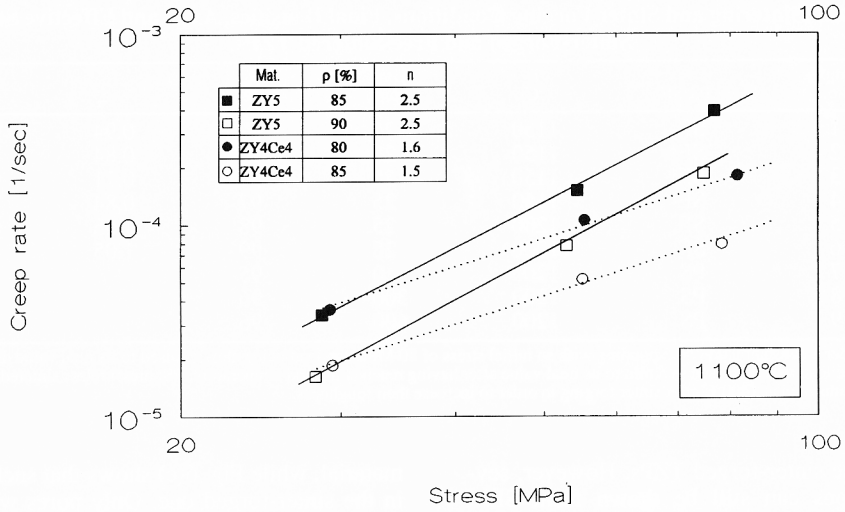

Fig. 4. Stress dependence of the creep strain rate of ZY5 at 85% and 90% relative density and of ZY4Ce4 at 80% and 85% relative density.

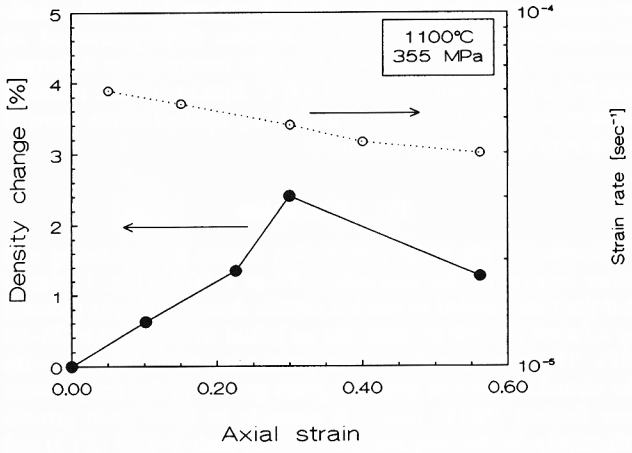

Fig. 5. The change in density $\Delta\rho/\rho_0$ as a function of axial strain during compressive deformation of ZY5 at 1100°C under 355 MPa initial stress. The starting density of the samples was 95.0% ± 0.4% of theoretical. Observed strain rates are also shown.

can be used to minimize the grain boundary resistance as indicated by Chen *et al.*,[19] who observed that the specific resistance of the grain boundaries in sinter-forged Y-TZP decreases strongly with increasing applied stress. The compressive stresses acting on the grain boundaries during sinter forging suppress the formation of a continuous, poorly conducting glassy film (originating from impurities such as Al_2O_3 and SiO_2) along these grain boundaries and decrease the grain boundary resistance in this way.

During sinter forging of ZY5 at 1100°C, theoretical densities could not be obtained. SEM analysis showed that one reason is the inability to completely eliminate flaws at this temperature. The "cavitation experiments," as described in Section III(3), indicate that a second reason might be the nucleation of cavities at large compressive strains.

The creep behavior of the sinter-forging ZY5 material can be compared with the results from creep tests performed on a dense ($\rho \geq 97\%$) 2.6Y-TZP material[16] with a grain size of 0.2 μm. The impurity contents of the two powder batches used were quite similar. For the dense material, a stress exponent equal to 2.2 has been determined at 1100°C–1300°C in the stress interval 16–120 MPa. This value is in fairly good agreement with the creep stress exponent found in this analysis ($n = 2.5$). The creep behavior of the dense ZY5 material has been interpreted as interface reaction controlled grain boundary sliding, in good agreement with the deformation map proposed by Nauer and Carry.[20] The precise character of the interface reaction is still a matter of debate. The value of the creep stress exponent determined for sinter forging suggests that the same mechanism is operating in porous Y-TZP with grain sizes near 0.1 μm ($\sigma = 28$–77 MPa, $T = 1100$°C). It is indeed expected from the deformation map that, for 0.1-μm grain size, creep is interface reaction controlled under the investigated experimental conditions.

The value of the creep stress exponent ($n \approx 1.5$) observed during sinter forging of ZY4Ce4 at 1100°C is in fairly good agreement with the n-value (1.8) determined from a creep test performed at 1200°C on a dense specimen. This n-value seems to be more representative of grain boundary diffusion control. More information from creep tests of dense YCe-TZP is, however, needed to establish which deformation mechanism is operating under the investigated experimental conditions.

The creep rates of ZY5 are higher than those of ZY4Ce4 during sinter forging (this result is corroborated by the hot forging tests performed on both materials). During sinter forging, ZY5 densifies faster than ZY4Ce4, while the reverse is true during free sintering. This indicates that plastic deformation is governing densification of the investigated materials during sinter forging. Other researchers have also found evidence for the important role of creep during pressure sintering of ceramics. Sheppard[21] pointed out that the addition of a deviatoric stress component greatly accelerates densification of alumina, compared to HIPing where the stress field is hydrostatic. Kellett and Lange[18] concluded that plastic deformation is the dominant mechanism for pore closure during hot forging of ZTA (the creep stress exponent of this material has a similar value[22] as observed here for TZP).

Panda *et al.*[23] have analyzed the sinter-forging characteristics of 2.9Y-TZP (Tosoh, Japan) at 1400°C in Ar, using constant piston velocities. They also observed a nonlinear stress dependence of both densification and creep rate. The creep stress exponent equals 3 at 80% and 95% relative density in their analysis. This value of the creep stress exponent plus the fact that the volumetric strain seems to be correlated with the effective strain only (irrespective of the applied stress) make them suggest that a dislocation type of plastic flow is responsible for densification. Comparing their analysis to ours, we see that the value of their creep stress exponent is somewhat higher: 3 compared to 2.5. More important, in our experiments the volumetric strain is not only related to the creep strain, but depends clearly on the applied stress (see Fig. 3). The observed differences in sinter-forging characteristics of both Y-TZP materials

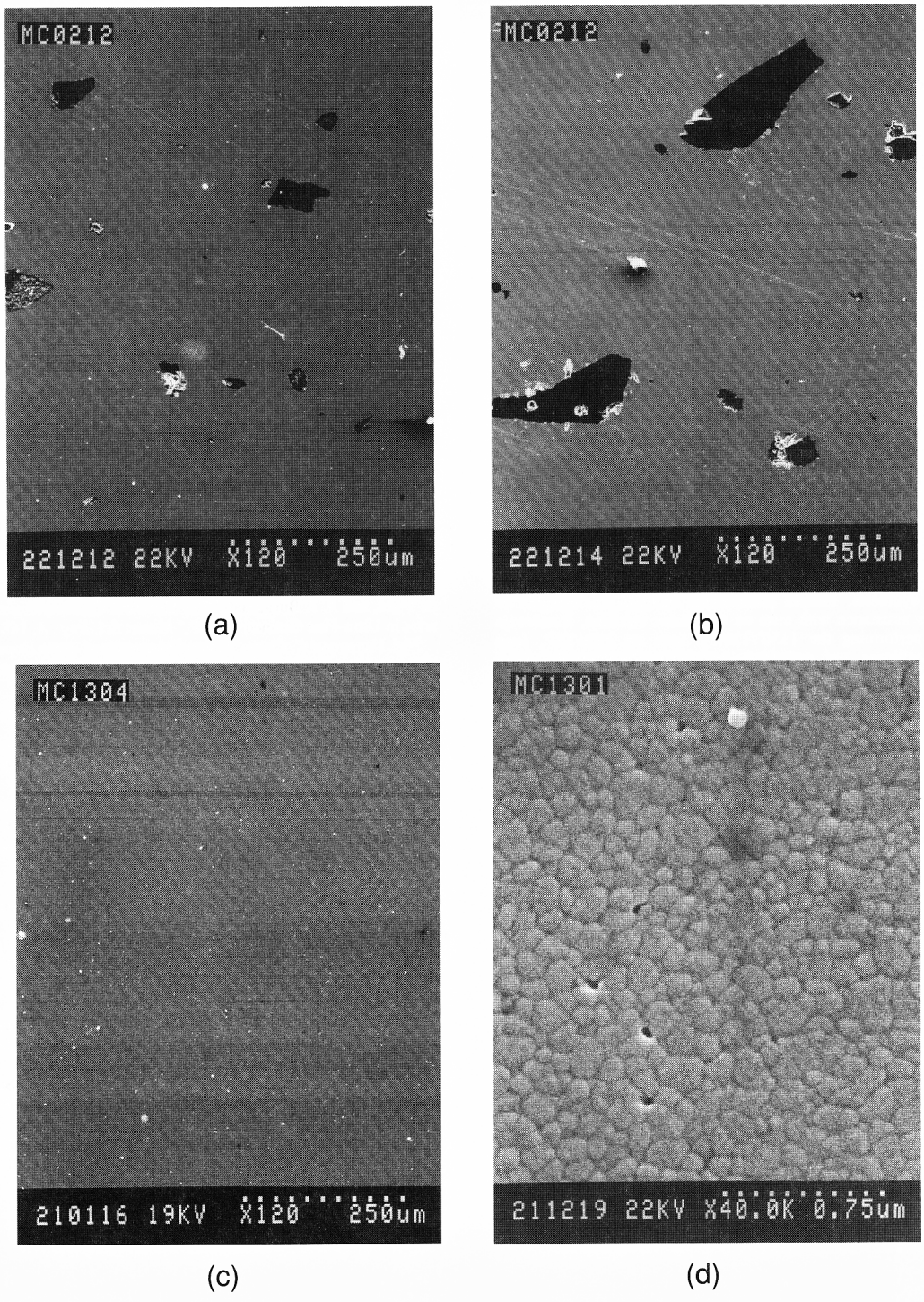

Fig. 6. Representative micrographs of Y-TZP: (a,b) free sintered at 1150°C for 10 h (97% dense) and (c,d) sinter forged at 1150°C under 80 MPa for 25 min (99% dense).

can possibly be related to differences in grain boundary chemistry. The composition of the amorphous silicate phase, virtually always present in Y-TZP materials, and the extent in which it wets the grain boundaries profoundly influence both creep[16,24,25] and densification.[26,27] Both atmosphere (Ar compared to air), temperature (1400°C compared to 1100°C), and total impurity content of the investigated materials differ markedly in comparing the analysis of Panda *et al.* with ours, and this will lead to strong differences in grain boundary chemistry[28,29,30] of both materials.

V. Conclusions

(a) Using sinter forging as a pressure-assisted densification technique for Y-TZP and YCe-TZP leads to a strong reduction of sintering time compared to free sintering.

(b) Nanostructured (grain size 0.10 μm) Y-TZP and YCe-TZP with high relative densities (90%–93%) could be obtained by sinter forging of the chloride materials under an initial stress of 84 MPa at 1100°C.

(c) In the last stage of sintering, the average size of flaws and residual pores decreases with increasing applied load

(accompanied by an increasing creep strain) in the materials sinter forged at 1100°C. Flaws could not be completely eliminated at this temperature.

(d) Near-theoretical (97%–99%) densities could be obtained with the investigated TZPs by sinter forging for 25 min at 1150°–1200°C under an initial stress of 80 MPa. Only pores with sizes smaller than the mean grain size (D = 0.18–0.25 μm) were observed in these materials, while the residual porosity (3%–5%) in free-sintered materials consists mainly of pores with sizes (up to 250 μm) and much larger than the mean grain size ($D \approx 0.2$ μm). Sinter forging at these temperatures offers the possibility to significantly improve final mechanical properties, compared to free sintering.

(e) Both the densification and creep rate of Y-TZP show a nonlinear relationship with the applied stress during sinter forging at 1100°C. The creep stress exponent determined in this analysis (n = 2.5) is in good agreement with the one determined from creep tests on dense samples of identical composition. This seems to indicate that the same mechanism—interface reaction controlled creep—is rate limiting, irrespective of the presence of porosity (maximum 15 vol% here). Observed creep rates were 10^{-4} s^{-1} under 80 MPa at 1100°C.

Acknowledgments: René Olde Scholtenhuis is gratefully acknowledged for powder synthesis, sample preparation, transport of samples to Switzerland, and his assistance with tests on the Elatec machine, Boudewijn van Langerak for performing the 1150°/1200°C tests on YCe-TZP, Joop Snoeyenbos for machining and polishing, and Marc Smithers for SEM observations.

References

[1]R. Raj, "Analysis of the Sintering Pressure," *J. Am. Ceram. Soc.*, **70** [9] C-210–C-211 (1987).

[2]R. L. Coble, "Diffusion Models for Hot Pressing with Surface Energy and Pressure Effects as Driving Forces," *J. Appl. Phys.*, **41** [12] 4798–807 (1970).

[3]R. K. Bordia and R. Raj, "Analysis of Sintering of a Composite with a Glass or Ceramic Matrix," *J. Am. Ceram. Soc.*, **69** [3] C-55–C-57 (1986).

[4]K. Venkatachari and R. Raj, "Enhancement of Strength through Sinter Forging," *J. Am. Ceram. Soc.*, **65** [3] 514–20 (1987).

[5]B. Budiansky, J. W. Hutchinson, and S. Slutsky, "Void Growth and Collapse in Viscous Solids"; pp. 13–45 in *Mechanics of Solids*. Edited by H. G. Hopkins and M. J. Sewell. Pergamon Press, New York, 1982.

[6]P. M. Hazzledine and J. H. Schneibel, "Diffusion-Accommodated Grain Boundary Sliding in a Polycrystal"; pp. 15–20 in *Superplasticity in Metals, Ceramics and Intermetallics*, MRS Symposium Proceedings, Vol. 196. Edited by M. J. Mayo, M. Kobayashi, and J. Wadsworth. Materials Research Society, Pittsburgh, PA, 1990.

[7]A. J. A. Winnubst, Y. J. He, P. M. V. Bakker, R. J. M. Olde Scholtenhuis, and A. J. Burggraaf, "Sinter Forging as a Tool for Improving the Microstructure and Mechanical Properties of Zirconia Toughened Alumina"; pp. 284–91 in Proceedings of *The Fifth International Conference on the Science and Technology of Zirconia*. Edited by S. P. S. Badwal, M. J. Bannister, and R. H. J. Hannink. Technomic, Lancaster, PA, 1993.

[8]M. M. R. Boutz, A. J. A. Winnubst, and A. J. Burggraaf, "The Effect of Ceria-Codoping on Chemical Stability and Fracture Toughness of Y-TZP," *J. Mater. Sci.*, in press.

[9]R. Raj, "Separation of Cavitation-Strain and Creep-Strain during Deformation," *J. Am. Ceram. Soc.*, **65** [3] C-46 (1982).

[10]W. F. M. Groot Zevert, A. J. A. Winnubst, G. S. A. M. Theunissen, and A. J. Burggraaf, "Powder Preparation and Compaction Behaviour of Fine Grained Y-TZP," *J. Mater. Sci.*, **25**, 3449–55 (1990).

[11]K. D. Debschütz, B. Caspers, G. A. Schneider, and G. Petzow, "Critical Evaluation of the Compression Creep Test," *J. Am. Ceram. Soc.*, **76** [10] 2468–74 (1993).

[12]J. C. Wurst and J. A. Nelson, "Lineal Intercept Technique for Measuring Grain Size in Two-phase Polycrystalline Ceramics," *J. Am. Ceram. Soc.*, **55**, 109 (1972).

[13]M. N. Rahaman, L. C. de Jonghe, and R. J. Brook, "Effect of Shear Stress on Sintering," *J. Am. Ceram. Soc.*, **69** [1] 53–58 (1986).

[14]Y. J. He, A. J. A. Winnubst, H. Verweij, and A. J. Burggraaf, "Sinter Forging of Zirconia Toughened Alumina," *J. Mater. Sci.*, in press.

[15]M. M. R. Boutz, A. J. A. Winnubst, and A. J. Burggraaf, "Yttria, Ceria Stabilized Tetragonal Zirconia Polycrystals. Sintering, Grain Growth and Grain Boundary Segregation," *J. Eur. Ceram. Soc.*, **13** [2] 89–102 (1994).

[16]M. M. R. Boutz, A. J. A. Winnubst, A. J. Burggraaf, M. Nauer, and C. Carry, "Low Temperature Superplastic Flow of Y-TZP," *J. Eur. Ceram. Soc.*, **13** [2] 103–11 (1994).

[17]M. M. R. Boutz, R. J. M. Olde Scholtenhuis, A. J. A. Winnubst, and A. J. Burggraaf, "A Hydrothermal Route for Production of Dense, Nanostructured Y-TZP," *Mater. Res. Bull.*, **29**, 31–40 (1994).

[18]B. J. Kellett and F. F. Lange, "Experiments on Pore Closure during Hot Isostatic Pressing and Forging," *J. Am. Ceram. Soc.*, **71** [1] 7–12 (1988).

[19]C. S. Chen, M. M. R. Boutz, B. A. Boukamp, A. J. A. Winnubst, K. J. de Vries, and A. J. Burggraaf, "The Electrical Characterization of Grain Boundaries in Ultra-Fine Grained Y-TZP," *Mater. Sci. Eng., A*, **168**, 231–34 (1993).

[20]M. Nauer and C. Carry, "Creep Parameters of Yttria Doped Zirconia Materials and Superplastic Deformation Mechanisms," *Scr. Metall. Mater.*, **24** [8] 1459–63 (1990).

[21]L. M. Sheppard, "The Evolution of HIP Continues," *Am. Ceram. Soc. Bull.*, **71** [3] 313–27 (1992).

[22]B. J. Kellett and F. F. Lange, "Hot Forging Characteristics of Fine-Grained ZrO_2 and Al_2O_3/ZrO_2 Ceramics," *J. Am. Ceram. Soc.*, **69** [8] C-172–C-173 (1986).

[23]P. C. Panda, J. Wang, and R. Raj, "Sinter-Forging Characteristics of Fine-grained Zirconia," *J. Am. Ceram. Soc.*, **71** [12] C-507–C-509 (1988).

[24]C. Carry, "Microstructures, Grain Boundaries and Superplasticity in Fine Grained Ceramics"; see Ref. 6, pp. 313–23.

[25]Y. Yoshizawa and T. Sakuma, "Role of Grain-Boundary Glass Phase on the Superplastic Deformation of Tetragonal Zirconia Polycrystal," *J. Am. Ceram. Soc.*, **73** [10] 3069–73 (1990).

[26]M. M. R. Boutz and P. den Exter; unpublished work.

[27]M. L. Mecartney, "Influence of an Amorphous Second Phase on the Properties of Yttria-Stabilized Tetragonal Zirconia Polycrystal," *J. Am. Ceram. Soc.*, **70** [1] 54–58 (1987).

[28]S. P. S. Badwal and A. E. Hughes, "The Effects of Sintering Atmosphere on Impurity Phase Formation and Grain Boundary Resistivity inY_2O_3-Fully Stabilized ZrO_2," *J. Eur. Ceram. Soc.*, **9**, 115–22 (1992).

[29]S. P. S. Badwal, J. Drennan, A. E. Hughes, and B. A. Sexton, "A Study of Impurity Phase Segregation in Fully Stabilized Yttria–Zirconia," *Mater. Sci. Forum*, **34–36**, 195–99 (1988).

[30]A. E. Hughes and S. P. S. Badwal, "Impurity and Yttrium Segregation in Yttria–Tetragonal Zirconia," *Solid State Ionics*, **46**, 265–74 (1991). □